Journal of Neuroscience Research 93:1388–1398 (2015)

Deimination Level and Peptidyl Arginine Deiminase 2 Expression Are Elevated in Astrocytes With Increased Incubation Temperature

Mabel Enriquez-Algeciras,[1,2] Sanjoy K. Bhattacharya,[1] and Horacio M. Serra[2]*

[1]Department of Ophthalmology, Bascom Palmer Eye Institute, University of Miami, Miami, Florida
[2]CIBICI, Department of Clinical Biochemistry, Faculty of Chemistry, National University of Córdoba, Córdoba, República Argentina

Astrocytes respond to environmental cues, including changes in temperatures. Increased deimination, observed in many progressive neurological diseases, is thought to be contributed by astrocytes. We determined the level of deimination and expression of peptidyl arginine deiminase 2 (PAD2) in isolated primary astrocytes in response to changes on either side (31°C and 41°C) of the optimal temperature (37°C). We investigated changes in the astrocytes by using a number of established markers and accounted for cell death with the CellTiter-Blue assay. We found increased expression of glial fibrillary acidic protein, ALDH1L1, and J1-31, resulting from increased incubation temperature and increased expression of TSP1, S100β, and AQP4, resulting from decreased incubation temperature vs. optimal temperature, suggesting activation of different biochemical pathways in astrocytes associated with different incubation temperatures. Mass spectrometric analyses support such trends. The PAD2 level was increased only as a result of increased incubation temperature with a commensurate increased level of deimination. Actin cytoskeleton and iso[4]LGE, a lipid peroxidase modification, also showed an increase with higher incubation temperature. Altogether, these results suggest that temperature, as an environmental cue, activates astrocytes in a different manner on either side of the optimal temperature and that increase in deimination is associated only with the higher temperature side of the spectrum.

Key words: peptidyl arginine deiminase; deimination; astrocytes; activation markers; temperature incubation; environmental cues

Astrocytes respond to environmental cues, including physicochemical stimuli, such as temperature, pressure, lack of oxygen, and hydrogen ion concentration, and biochemical stimuli, such as cytokines and other biological signals. The responses of astrocytes are often designed to protect the neuronal system from damage or to promote repair after injury (Ridet et al., 1997). A greater understanding of the effects of these stimuli in an integrated fashion for the whole body will provide insight into the effects of different factors in normal function as well as their aberration in diseased states.

Physiochemical factors, such as pressure, hypoxia, and pH and temperature changes, have been shown to have greater specific effects in certain neurological diseases than in others. For example, intraocular pressure is critical to the development of irreversible blinding neurological diseases such as glaucoma (Ahmed et al., 2001) and pressure and hypoxia are associated with different types of neurological strokes (Sambandam et al., 2004; Zhang et al., 2014). Exposure to either side of the spectrum of temperature from the optimal temperature may result in trauma to the neuronal system. For example, a significant proportion of individuals suffering from multiple sclerosis (MS) experience worsening of neurological symptoms as a result of elevated body temperature. A rise in temperature induced by exercise has been noted to worsen neurological conditions in these patients (Guthrie and Nelson, 1995). Subjecting patients to a transient rise in temperature up to 40°C (hyperthermia) was found to have some temporary beneficial effects. However, this also has been linked to severe neurological complications; therefore, the practice is no longer used (Berger and Sheremata, 1982). Conversely, therapeutic hypothermia (controlled reduction of a patient's core temperature below 36°C; Polderman and Herold, 2009) is widely used after traumatic brain injury, with beneficial effects. The central nervous system (CNS) has many different types of cells performing vastly different functions. These cells respond to physiochemical and biochemical cues differently.

*Correspondence to: Horacio Serra, CIBICICONICET, Departamento de Bioquímica, Clínica Facultad de Ciencias Químicas, Universidad Nacional de Córdoba, Haya de la Torre esquina Medina Allende, Ciudad Universitaria, 5016 Córdoba, República Argentina.
E-mail: hserra@fcq.unc.edu.ar

Received 27 August 2014; Revised 20 February 2015; Accepted 26 February 2015

Published online 20 March 2015 in Wiley Online Library (wileyonlinelibrary.com). DOI: 10.1002/jnr.23587

Astrocytes are the most abundant cell type in the CNS, becoming activated in response to many CNS pathologies, such as stroke, trauma, and neurodegenerative diseases (Pekny and Nilsson, 2005). Astrocytes have been shown to be a major source of inflammatory cytokines, such as interleukin-6 and tumor necrosis factor-α, after brain injury (Gruol and Nelson, 1997; Martin et al., 2001).

Deimination refers to the conversion of protein-bound arginines into protein–citrullines catalyzed by a family of enzymes called peptidyl arginine deiminases (PADs). It is a long term, irreversible posttranslational modification that is catalyzed principally by PAD2 in the CNS (Vossenaar et al., 2003; Mowen and David, 2014). Elevated deimination has been associated with CNS tissues in neurodegenerative diseases such as MS, glaucoma, and Alzheimer's disease (Wood et al., 1996; Bhattacharya et al., 2006b; Nicholas, 2013; Bradford et al., 2014). Astrocytes have been the cell type to which elevated deimination has largely been attributed (Enriquez-Algeciras et al., 2013). The effect of mechanical stress and hydrostatic pressure on astrocytic deimination has been previously investigated (Yu et al., 2004; Algeciras et al., 2008). However, the effect of temperature on astrocytic deimination remains to be studied. Understanding the responses of individual cell types with respect to isolated physicochemical parameters will help in deciphering the precise contribution of the cells to integrative responses of the organ and eventually the organism. However, to dissect the responses of individual cell types within the milieu of tissue or in a mixed batch of cells is extremely difficult. Isolated and enriched cell culture offers insight into the effect of such parameters. Astrocytes, the most numerous kind of glial cell in the brain, are normally considered to have a supportive role to neurons. However, it is now accepted that astrocytes function as key players, participating in synaptic formation and aiding in tissue repair. When exposed to trauma or pathological conditions, astrocytes become activated, a process known as *reactive gliosis/activation*.

Astrocytes are thought to undergo activation in response to environmental temperature fluctuation. However, whether the underlying biochemical pathways or protein expression as well as deimination is uniformly activated on either side of the optimal growth temperature has not been investigated. This study presents our experimental results of changes in established astrocyte markers, PAD2, and deimination in astrocytes subjected to exposure to temperatures on either side of the optimal temperature.

MATERIALS AND METHODS

Tissue Preparation

Astrocytes were isolated from surgically dissected cerebral cortex according to published methods (Gregorios et al., 1985). Briefly, cortices were dissected from 7-day-old C57/Bl6 mice, making sure to remove the meninges and blood vessels. Tissue pieces of about 1 mm^3 were transferred to a 15-ml centrifuge tube. The minced tissue was incubated with 0.25% trypsin/EDTA solution at 37°C for 10 min. Digestion was stopped by adding Dulbecco's modified Eagle's medium + 10% fetal bovine serum; (FBS) + 40 μg/ml gentamicin, and the tissue homogenate was plated onto poly-L-lysine-coated eight-chamber slides (Nunc, Rochester, NY). The medium was changed regularly, and, after 10 days, when the cell layers became stable, the medium was changed to one containing horse serum instead of FBS. At this stage, most cells were astrocytes. The microglia were removed from this mixed culture by incubating with 0.5 mM dibutyryl cAMP after day 14 to yield >95% pure astrocyte cultures. Cells were expanded by replacing the medium once per week. Enrichment of astrocytes was confirmed by immunostaining with antibodies against Iba1, which stains microglia as well as macrophages, and glial fibrillary acidic protein (GFAP), a marker of astrocytes.

Astrocytes (1×10^5 cells/well) were cultured on top of an 18-mm-circle microcover glass inside 12-well plates. Cells were divided into three groups, each with an incubation of 1 hr at 31°C, 37°C, or 41°C, followed by a stabilization period of 24 hr at normal temperature (37°C). The cell culture incubators were checked to make sure that there was no variability in temperature during the 1-hr treatment. All animal experiments were performed according to protocols approved by the Institutional Animal Care and Use Committee at the University of Miami.

Cell Viability

Cell viability was measured with the CellTiter-Blue assay (Promega, Madison, WI) by adding the CellTiter-Blue reagent to the wells (20 μl reagent to each 100 μl medium in a 96-well plate) for 4 hr, followed by quantification with an ELISA plate reader. The manufacturer's protocol was followed by measuring fluorescence as readout at 590 nm. Cell viability was compared among treatments and normalized to that of untreated cells. Triplicate wells without cells served as negative controls to determine background fluorescence.

Immunohistochemistry

The cells were subsequently fixed in 4% paraformaldehyde on coverslips for 30 min, permeabilized with 0.2% Triton X-100 in 1× phosphate-buffered saline (PBS) for an additional 30 min, and blocked in PBS containing 0.2% bovine serum albumin (BSA). Labeling of the cells was performed with antibodies selected from the literature as being expressed in reactive astrocytes. Briefly, they were probed with antibodies for GFAP (mouse monoclonal; BD Biosciences Pharmingen, San Diego, CA), aquaporin-4 (AQP4; goat polyclonal; Santa Cruz Biotechnology, Santa Cruz, CA), rabbit polyclonal anti-iso[4]-LGE2 (Govindarajan et al., 2009), monoclonal antibody against recombinant PAD2 (Koike et al., 1994), anti-ALDH1L1 antibody–astrocyte marker (rabbit polyclonal; Abcam, Cambridge, MA; Foo and Dougherty, 2013; Boesmans et al., 2014), anti-glutamine synthetase (rabbit polyclonal; Sigma-Aldrich, St. Louis, MO), antiastrocytomas low-grade antibody (J1-31; mouse monoclonal; Abcam; Predy et al., 1988; Malhotra et al., 1995; Garcia et al., 2003; Shuangshoti et al., 2009), anti-S100β protein (mouse monoclonal, clone 4C4.9; EMD Millipore,

Billerica, MA), thrombospondin (TSP1; mouse monoclonal; Abcam), antipeptidyl–citrulline IgM, clone F95, for direct measurement of citrullination (mouse monoclonal; Millipore), and anticonnexin 43 (Cx43; mouse monoclonal; Invitrogen, Carlsbad, CA). The secondary antibodies, anti-mouse, anti-rabbit, or anti-goat, were coupled with fluorescein isothiocyante (FITC), Alexa 594, or Cy5. After incubation with secondary antibodies, the cells were stained with 4′,6-diamidino-2-phenylindole (DAPI) for 45 min. The cells were stained with phalloidin (rhodamine–phalloidin; 1:100 dilution in 1× PBS for 5 min) to observe changes in the actin filaments. After staining of the cells, the coverslips were inverted and placed on slides, sealed with Vectashield (Vector Laboratories, Burlingame, CA), and subjected to confocal microscopy on a Leica (Exton, PA) TCS-SP5 laser scanning confocal microscope. Negative controls consisted of cells incubated with secondary antibody alone. For confocal image quantification, the area for measurement was demarcated in ImageJ, allowing normalization of the area parameter. The intensity of the DAPI signal was used for deriving a normalizing intensity factor, which was applied to other signals measured.

Quantitation

For Western blotting, proteins extracted from astrocyte cultures (10 μg) were resolved by SDS-PAGE on 4–20% gradient gels, transferred to a polyvinylidene fluoride membrane, and blocked overnight in 5% nonfat milk. Membranes were probed with monoclonal antibody against PAD2 (a research gift from Prof. Hidenari Takahara, Ibaraki University, Ibaraki, Japan; Takahara et al., 1989; Terakawa et al., 1991). The other antibodies were GFAP (mouse monoclonal; BD Biosciences Pharmingen), AQP4 (goat polyclonal; Santa Cruz Biotechnology), rabbit polyclonal anti-iso[4]LGE2 (Salomon et al., 1999), anti-ALDH1L1, an astrocyte marker (rabbit polyclonal; Abcam), antiglutamine synthetase (rabbit polyclonal; Sigma-Aldrich), antiastrocytomas low-grade antibody (J1-31; mouse monoclonal; Abcam), Slit1 (rabbit polyclonal; Abcam), TSP1 (mouse monoclonal; Abcam), and antipeptidyl citrulline IgM, clone F95, for direct measurement of citrullination (mouse monoclonal; Millipore). Primary antibody–antigen complex was detected with an appropriate secondary antibody. Proteins were visualized with a chemiluminescence kit (ECL; GE Healthcare, Piscataway, NJ). Blots were probed with glyceraldehyde-3-phosphate dehydrogenase (GAPDH; mouse monoclonal; Chemicon, Temecula, CA) as a loading control. Western blot images were scanned, and intensities were determined in ImageJ. $P < 0.05$ was considered statistically significant. Quantitative Western blotting results were confirmed with IR-700 dye-coupled secondary antibody (nonamplified signal capture) in the Odyssey infrared imaging system (LI-COR Biosciences, Lincoln, NE).

For quantification of image fluorescence, a group consisting of three independent observers recorded the intensity of the fluorescence on a scale of 1–10, where 1 was weakest fluorescence and 10 was the strongest fluorescence.

ELISA was also conducted. Briefly, plates with astrocytic proteins from the cultures were incubated (1:1,000) at 37°C for 1 hr. Then, the plates were blocked with 0.2% BSA in PBS and incubated at 37°C for 1 hr. The supernatant was discarded, and the plate was washed with PBS. Primary antibodies in 1:500 dilutions to anti-iso[4]LGE2, PAD2, GFAP, citrulline (F95), J1-31, ALDH1L1, S100β, and AQP4 were added, and the plates were incubated at room temperature for 1 hr. After that, the supernatant was discarded, and the plate was washed with PBS three times. Secondary antibody coupled with alkaline phosphatase was used for a 1-hr incubation. The plate was then washed with PBS, incubated with phosphatase substrate (100 μl/well) in diethanolamine buffer (pH 7.5), and quantified at 405 nm on a plate reader (BioTek Synergy HT; BioTek Instruments, Winooski, VT). A similar analysis was performed with a primary rabbit polyclonal GAPDH loading control antibody (Sigma-Aldrich). Immunoreactivity was normalized to GAPDH immunoreactivity.

Mass Spectrometry

For mass spectrometry analysis, protein bands separated on 4–20% SDS-PAGE were excised and subjected to gel digestion. Briefly, protein bands were destained with HPLC-grade acetonitrile and water (1:1) and 100 mM ammonium bicarboante (HPLC-grade water), reduced with dithiotheritol, and alkylated with iodoacetamide. Proteins were isolated with sequencing-grade trypsin (0.1 μg/20 μl N-ethyl morpholine), pulled out with three washes (twice with HLPC-grade acetonitrile and water [1:1] and once with HPLC-grade pure acetonitrile), and then subjected to speed-vaccing to dry the proteins to prepare for mass spectrometry analysis. Resulting peptides were loaded onto an analytical Betabasic C18 capillary chromatography column (2.1 × 100 mm) packed with 3 μm C18 reversed-phased resin (Pierce Biotechnology, Rockford, IL). Peptides were ionized and eluted into a linear ion trap according to the following linear HPLC gradient: 0–20 min A (15%), B (85%); 20–25 min A (5%) and B (95%); conditions were held from 25 to 43 min; then 43–47 min A (97%) and B (3%) going to initial conditions at a flow rate of 250 μl/min (mobile phase A: 100% water/0.1% formic acid; mobile phase B: 100% acetonitrile/0.1% formic acid). Spectra were acquired with a Q-Exactive mass spectrometer (Thermo Fisher Scientific, Waltham, MA). During LC-tandem mass spectrometry (MS/MS) analysis, the mass spectrometer performed data-dependent acquisition with a full mass spectrometry scan between 450 and 1800 m/z, followed by three MS/MS scans (30% collision energy) on the three most intense ions from the preceding mass spectrometry scan. Data acquisition was performed by using dynamic exclusion with a repeat count of 2 (for 30-sec repeat duration) and a 45-sec exclusion duration window. All MS/MS spectra were searched (Mascot; Matrix Science, Boston, MA) in Swiss Prot database. Searches of database entries were unrestricted and allowed a maximum of two missed cleavages. These methods are well established in our laboratory (Parikh et al., 2011).

Statistical Analysis

All experiments were performed at least three times. Statistical analyses were performed in IBM SPSS version 21 (IBM, Armonk, NY). Results are reported as mean ± SEM for at least three independent experiments. Data were subjected to

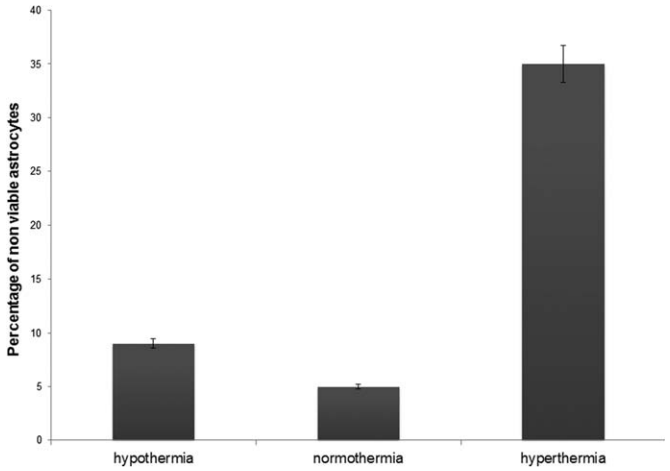

Fig. 1. Determination of cell viability with the CellTiter-Blue assay. Identical pools of astrocytes (n = 3,000) subjected to incubation at 31°C, 37°C, and 41°C (depicted as hypothermic, normothermic, and hyperthermic, respectively) for 1 hr were subjected to assessments of cell viability. The results are mean ± SEM from three independent experiments. *P* values were determined with Student's *t*-test and found to be nonsignificant. Percentage of nonviable cells was estimated from total number of cells used for initial plating.

Student's *t*-test or ANOVA, followed by post hoc least significant difference (LSD) testing. The level of statistical significance was set at $P < 0.05$.

RESULTS

The isolated and enriched astrocyte cells from a single pool grown at 37°C were divided into three groups for the following experiments. Each pool was subjected to an incubation of 1 hr at 31°C, 37°C, or 41°C, which was followed by a 24-hr stabilization period at 37°C. The rationale behind this experiment was to develop a quantitative estimate of the effect of environmental short-term exposure to temperatures outside normal on optimal growth and on the number of viable astrocytes. Although long-term exposure to isolated cells is expected to result in more nonviable cells, shorter exposure to temperature on either side of 37°C may or may not change the number of cells. A significant change in number of viable cells would contribute to deimination changes. To understand better and account for such changes, it was necessary to adopt this experimental design. This design is applicable to tissue and at the whole-organ level for determining whether a shorter temperature change in the outside world would result in a change in cell viability when the tissue, organ, or organism has subsequently been brought back to normal or optimal temperature. Identical astrocyte cell aliquots were utilized to probe for cell viability with incubation temperature by using the CellTiter-Blue assay (Fig. 1). We found that <5% of cells were nonviable at 37°C (normothermic condition), whereas 10% and 35% of cells were nonviable with exposure to 31°C (hypothermic) and 41°C (hyperthermic), respectively. Thus, only marginal loss of viability was observed under hypothermic conditions, whereas a substantial increase in nonviable cells was found to result from exposure to hyperthermic compared with normothermic conditions (Fig. 1). Only the live astrocytes (excluded by trypan blue assay) were used for immunohistochemical analyses.

Immunohistochemical analyses were performed with established biochemical markers and subjected to assessment of cellularity with nuclear staining, gross astrocytic morphology, actin filament staining, and assessment of GFAP independently for each pool of cells analyzed. GFAP serves as an activation marker for astrocytes; however, because each group of cells may undergo a different degree of activation and because of inherent variability in epitope exposure and degree of antigen–antibody reactivity, each pool and each panel was subjected to staining for GFAP and DAPI independently. Immunohistochemical analyses revealed greater fluorescence intensity for GFAP in cells subjected to 41°C than in those subjected to 37°C, and 31°C showed the lowest intensity for GFAP across all pools of the astrocyte cultures (Fig. 2). Intensity of phalloidin and lipid peroxidation product iso[4]LGE immunoreactivities showed a parallel trend, suggesting that the measure of activation by GFAP is commensurate with actin cytoskeleton expansion and accumulation of isolevuglandin peroxidation products (Fig. 2). The rationale for these experiments was to determine specific proteins that undergo significant alteration in expression resulting from temperature changes with simultaneous determination of their localizations.

Immunohistochemically, the astrocyte activation markers TSP, AQP4, and S100β showed an opposite spectrum pattern from GFAP and ALDH1L (Fig. 2). In fact, TSP, AQP4, and S100β showed increased fluorescence intensity at 31°C with progressive decrease at 37°C and 41°C; the exact opposite was true for GFAP and ALDH1L (Fig. 2).

To obtain a measure of how astrocyte function might be affected by different temperature incubations, we performed an assessment of gap communication function by staining with the gap junction protein Cx43. Although Cx43 is not a direct measure of astrogliosis or astrocyte reactivity, it can be used as a measure of gap function communication (Theodoric et al., 2012). We found that gap function communication was impaired or reduced at the high-temperature incubation (Fig. 3A).

Astrocyte processes contact many neural synapses per cell, and, to measure how temperature incubation might have affected the interaction with their surrounding environment, we measured the astrocytic process length. We found that only after the hypothermic treatment the length of the processes was significantly reduced compared with normothermic conditions (Fig. 3B). The rationale for these experiments was to determine some measurable cellular function in vitro that is affected by changes in environmental temperature.

PAD2 showed its lowest level at 31°C, with progressively increased levels at 37°C and 41°C. As expected, these results paralleled those for deimination, a measure of PAD2 activity (Fig. 2).

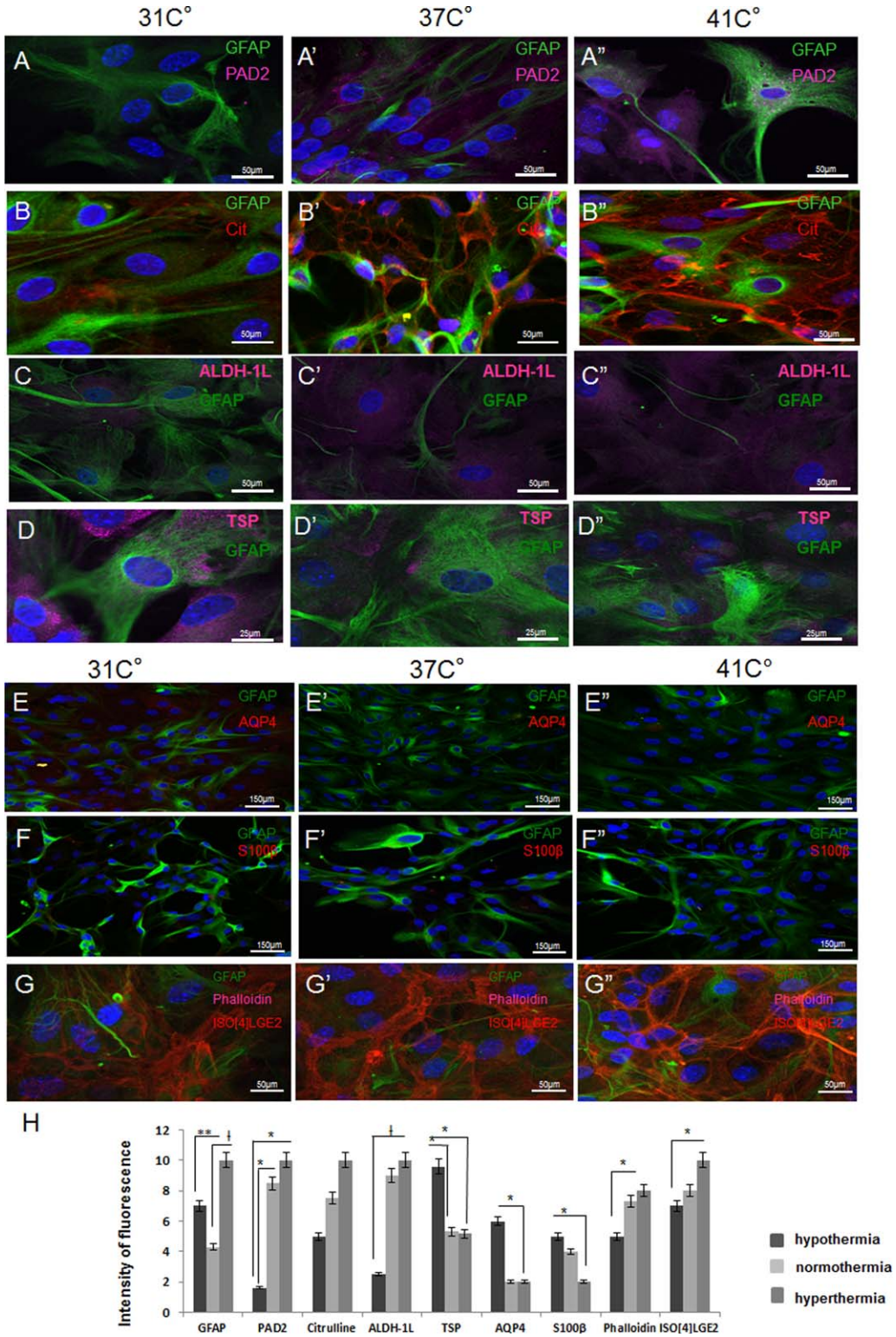

Fig. 2. Astrocytes evaluated for expression of activation markers, PAD2, and deimination as a consequence of incubation at optimal and suboptimal temperatures. Astrocytes were probed after 1 hr of incubation at the indicated temperatures. Immunohistochemical analysis used antibodies against the antigens indicated: GFAP (FITC) and double labeling with PAD2 (Cy5; **A,A′,A″**), anticitrulline (Alexa 594; **B,B′,B″**), anti-ALDH-1L (Cy5; **C,C′,C″**), and TSP1 (Cy5; **D,D′,D″**). Immunohistochemical analysis with antibodies against GFAP (FITC) and double labeling with AQP4 (Alexa 594; **E,E′,E″**), S100β (Alexa 594; **F,F′,F″**), and phalloidin (Cy5) and antiiso[4]LG2 (Alexa 594; **G,G′,G″**). **H:** Quantification of intensity of immunohistochemistry fluorescence as determined by three independent observers. Fluorescence was recorded on a scale of 1–10, with 10 = maximum fluorescence. Data were subjected to ANOVA, followed by post hoc LSD. Values are expressed as mean ± SEM from three independent experiments. $\star P < 0.05$, $\star\star P < 0.005$, $P < 0.001$. Scale bars = 50 μm in A–C″,G–G″; 25 μm in D–D″; 150 μm in E–F″. [Color figure can be viewed in the online issue, which is available at wileyonlinelibrary.com.]

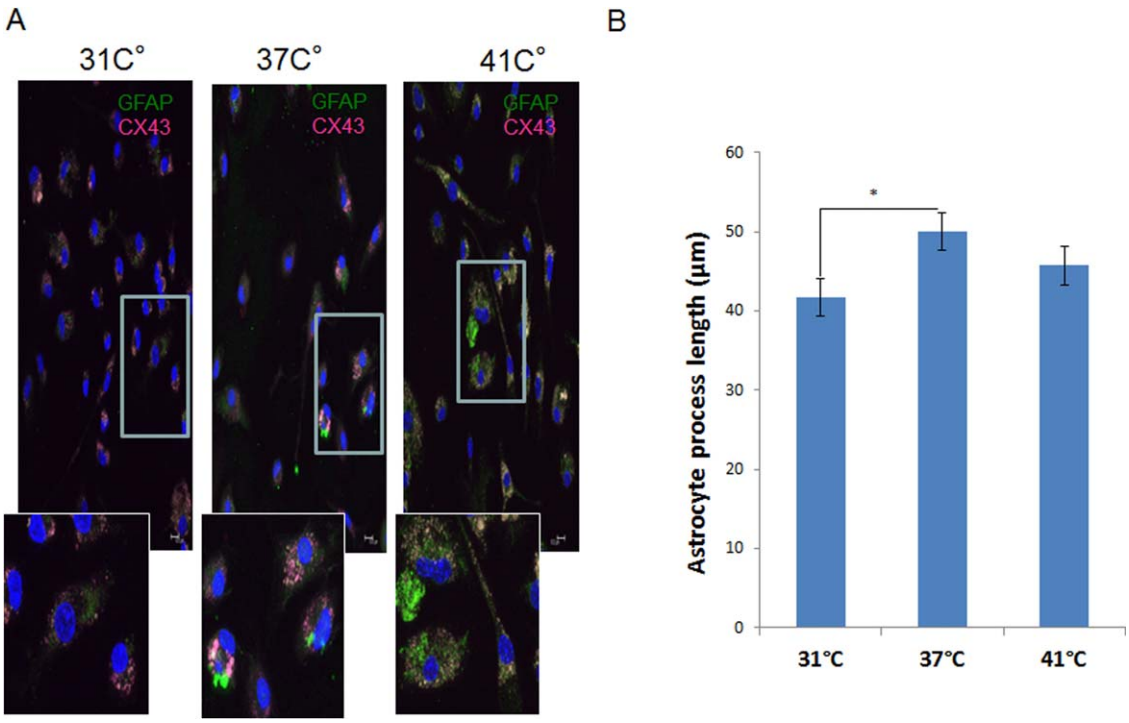

Fig. 3. Assessment of gap junction connectivity and astrocytic process length. **A:** Astrocytes were evaluated for expression of gap junction protein CX43 after incubation at optimal and suboptimal temperatures. Astrocytes were probed after 1 hr of incubation at the indicated temperatures. Immunohistochemical analysis used antibodies against indicated antigens: GFAP (FITC) and double labeling with CX43 (Cy5). Enlarged areas depict insets for each panel. **B:** Quantification of astrocyte process length after each temperature incubation period. Values are expressed as mean ± SEM from three independent experiments. Data were subjected to one-way ANOVA, followed by post hoc LSD. $\star P < 0.05$. Scale bars = 100 µm. [Color figure can be viewed in the online issue, which is available at wileyonlinelibrary.com.]

ELISA (Fig. 4A,B) and Western blot analyses (Fig. 4C,D) also showed the progressive increase in GFAP or ALDH1L and J1-31with an increase in temperature from 31°C to 41°C. Astrocytes are likely to undergo activation concomitant with increased metabolic activity from 31°C to 41°C. The increase in GFAP and ALDHL1 from 31°C to 41°C is consistent with activation of astroyctes and increased metabolism, respectively. Astrocyte activation is also associated with expansion of cell size; thus, a cytoskeletal protein such as J1-31 is expected to show an upregulation. A caveat is that J1-31 shares epitopes with GFAP, which is clearly upregulated on astrocyte activation; thus, the possibility that the current observations are due to overlapping GFAP epitopes (Garcia et al., 2003) cannot be entirely ruled out. A reverse trend was found for TSP, AQP4, and S100β, supporting the findings of semiquantitative immunohistochemistry (Fig. 2). Astrocytes subjected to trauma have been shown to demonstrate reduced intra- and extracellular TSP-1 and reduced AQP4 levels (Zhao et al., 2005; Nesic et al., 2006; Jayakumar et al., 2014), consistent with our observation of the same from the exposure to higher temperature. Reduced levels of AQP4 are usually associated with increased S100β secretion. For maintenance of overall constant level, it has been shown that, with some environmental parameters, increased secretion is consistent with decreased intracellular protein level for S100β, which is parallel to the higher temperature affecting astrocytes in a similar fashion (Zanotto et al., 2013).

PAD2 and deimination showed commensurate increases from 31°C to 41°C. The lowest temperature in this study also led to very little or basal levels of PAD2 and deimination. Quantification of both Western blots and immunofluorescence is presented in Figures 2H and 4E.

To investigate whether other proteins also show selective increased expression at 31°C, 37°C, or 41°C, we performed mass spectrometry analysis (Fig. 5), the results of which suggested that this indeed was the case. The DEP domain-containing protein 5 (DEPDC5) was found to have higher expression on either side of the optimal temperature of 37°C. At 37°C, the expression of DEPDC5 was minimal. On the other spectrum, there were some proteins that were associated only with normothermic conditions (37°C), such as dynein heavy chain 10, putative DNA helicase INO80 complex homolog 1, the small subunit processome component 20 homolog UTP20, and nucleosome-remodeling factor subunit BPTF.

Some of the proteins upregulated only during hyperthermic conditions were ankyrin 1 (Okada-Ogawa et al., 2009) and ATP-binding cassette subfamily A member 5 (Kim and Halliday, 2012), whereas some proteins, such as serine/threonine protein kinase SMG1 and CLIP-

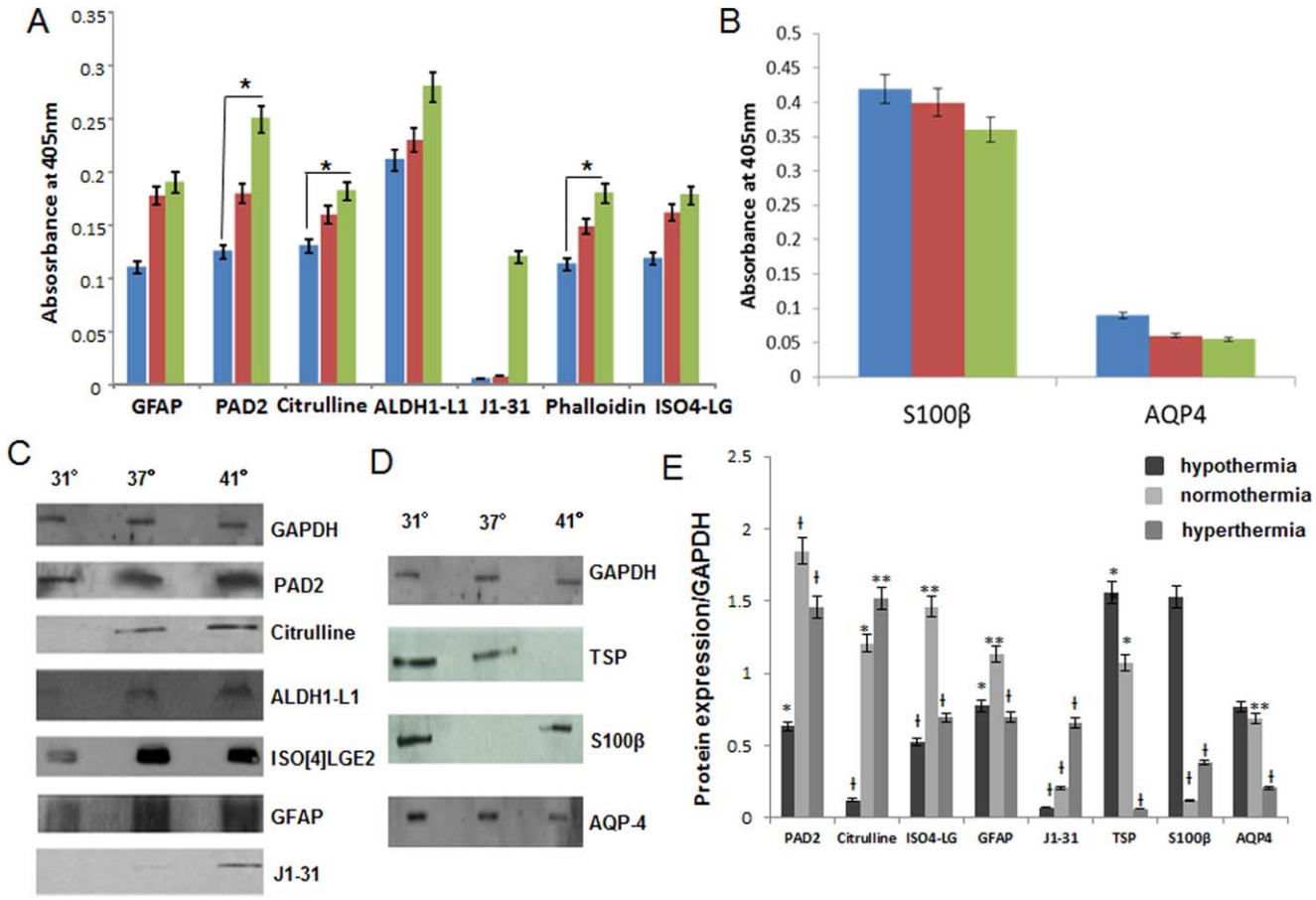

Fig. 4. Confirmation of level of activation markers, PAD2, and deimination with quantitative methods. **A:** ELISA analyses of astrocytes subjected to different-temperature incubation treatments: 31°C (blue bar), 37°C (red bar), and 41°C (green bar) with antibodies as indicated. **B:** ELISA analyses of astrocytes subjected to different temperature incubation as for A, with indicated antibodies. Values are expressed as mean ± SEM from three independent experiments. **C:** Western blot analyses of astrocyte extract (10 μg) probed with antibodies as indicated show astrocyte markers upregulated after hyperthermic treatment. **D:** Western blot analyses of astrocyte extract (10 μg) probed with antibodies as indicated show markers upregulated after hypothermic treatment. Data were subjected to ANOVA, followed by post hoc LSD. **E:** Quantification of Western blotting immunoreactivity (average of three readings) in ImageJ and normalized to GAPDH. After normalization, a two-tailed one-sample *t*-test was performed to compare each mean with the reference value of 1.0. Values are expressed as mean ± SEM. $\star P < 0.05$, $\star\star P < 0.005$, $P < 0.001$. [Color figure can be viewed in the online issue, which is available at wileyonlinelibrary.com.]

associating protein 1, were found to be highly expressed under hypothermic conditions (41°C). The proteins shown in Figure 5 fall basically into four broad categories: 1) transcription factors and/or DNA metabolizing proteins, 2) enzymatic proteins, 3) proteins associated with energy metabolism, and 4) proteins associated with cellular transport. Some sort of modulation in all of these categories is expected; for example, temperature should upregulate some and downregulate other transcription factors. The same would be applicable to DNA metabolizing enzymes, whose actions are associated with up- or downregulation of proteins, such as those associated with eu-heterochomatin formation. Many and varied enzymatic proteins are modulated beyond optimal temperature; for example, serine–threonine kinase is upregulated at lower than optimal temperature, potentially to increase signaling and survival. Transport-associated proteins, such as dynein, are downregulated on either side of optimal temperature, as would be expected. Energy metabolism proteins, such as succinate dehydrogenase and ATP-binding proteins, are upregulated at 41°C but not at lower temperatures. The upregulation of energy metabolism proteins suggests that more energy production is required to maintain homeostasis or synthesis of proteins and factors that nullify the deleterious effects of higher temperature exposure even for a short period. Many garbage-disposal enzymes, such as ubiquitin hydrolase, are also upregulated subsequent to short-term exposure to 41°C, perhaps to clear the aggregated or damaged proteins formed as a result of exposure to high temperature.

DISCUSSION

The central nervous system in mammals and humans is composed of many cell types that have different functions.

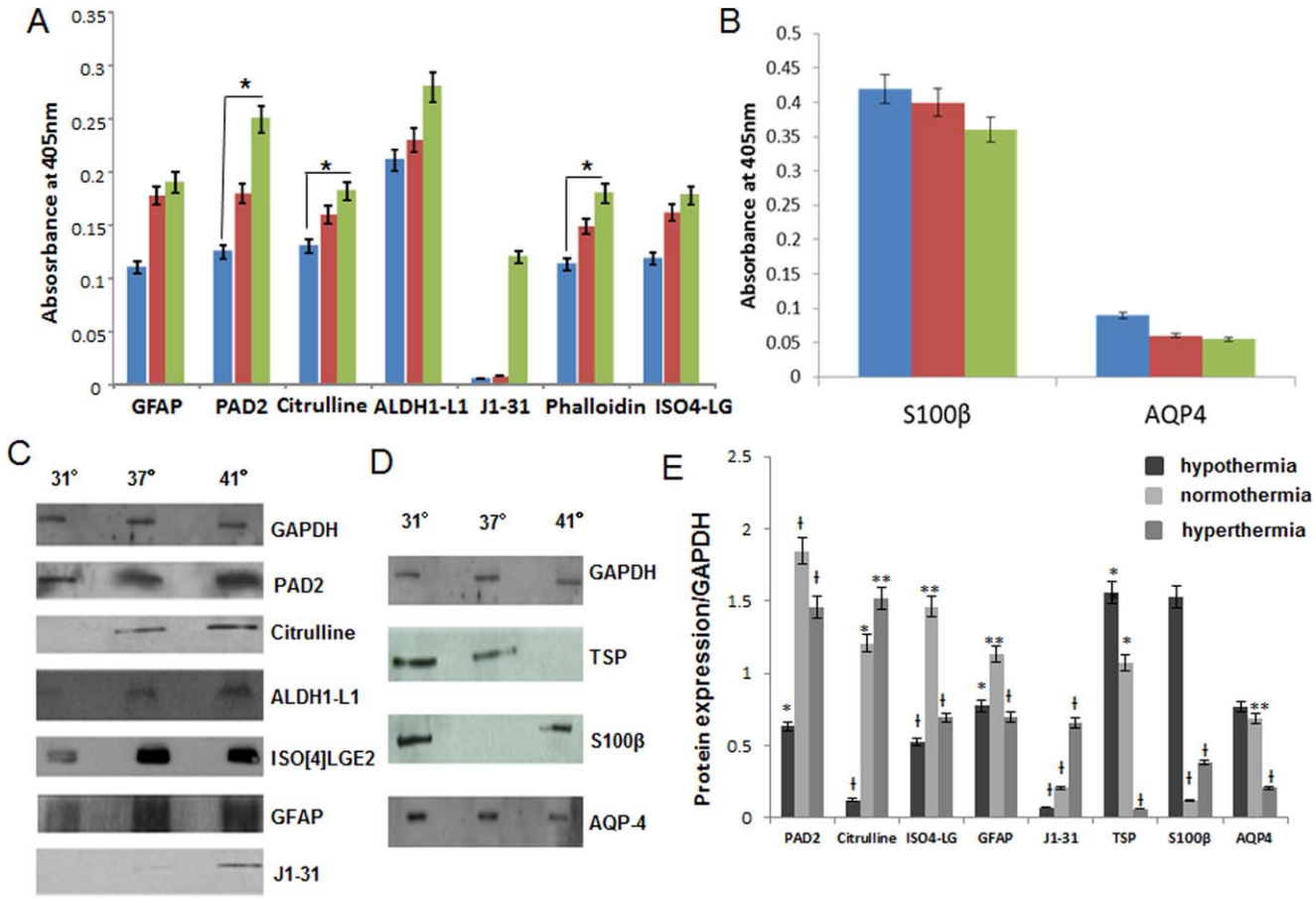

Fig. 5. Proteins identified by mass spectrometric analysis.

Astrocytes often serve as responders to environmental cues. They also play supporting and protective roles for neurons. The exact response to the environmental cues, such as environmental temperature or alteration in temperature, of astrocytes in the complex milieu of tissue is difficult to decipher. Either spectrum of optimal temperature has an effect on the cells. The effect of temperature is also realized on the whole body, particularly in pathologic or stress situations. For example, hyperthermia exacerbates frequency of spastic tremors in MS patients. Hypothermia applied almost immediately and locally brings about a beneficial effect on survival in traumatic brain or other neuronal injury. Hypothermia reduces cerebral oxygen consumption by a rate of approximately 6% per 1°C change in temperature, allowing preservation of potentially viable brain tissue for longer periods (Froehler and Ovbiagele, 2010; Wu and Grotta, 2013). Furthermore, free radical formation and inflammatory responses are inhibited during hypothermia (Globus et al., 1995). Hypothermia, on the other hand, has been found to be damaging under conditions such as cerebral ischemia, in which it causes neuronal damage and glial activation (Kim et al., 2014). Hyperthermia is also associated with conditions in which there is uncontrolled heat production, such as malignant hyperthermia, cerebral hemorrhage, and drug-induced hyperthermia, among others. Astrocytes are one of the prominent cell types responding to these temperature effects. We have previously shown the effect of mechanical stretch on PAD2 expression and deimination in astrocytes. Astrocytes and immature oligodendrocytes have been found to be major contributors to elevated and aberrant deimination following neuronal diseases (Akiyama et al., 1999; Bradford et al., 2014).

This study used isolated astrocytes from the cerebral cortex to examine the effects of temperature incubation in these cells. We speculate that results from these investigations will expand our understanding of what might occur in MS patients who have been exposed to excessive heat. Adverse effects, including increased frequency of spasm, have been documented in MS patients exposed to high heat or suboptimal heat for some duration (Guthrie and Nelson, 1995; Flensner et al., 2011). Astrogliosis and astrocyte reactivity are two of the hallmarks of this disease; therefore, we embarked on an investigation to determine whether there is a link between astrocyte reactivity and temperature in isolated astrocytes subjected to elevated-temperature incubation

treatments. Our in vitro analyses with two different approaches showed 37°C to be the optimal temperature, with a deviation from this temperature on either side being suboptimal for indirect estimate of intercellular communication and subcellular process formation. We used expression of CX43 as an indirect estimate of intercellular communication in astrocytes, as reported elsewhere (Theodoric et al., 2012); this was our first approach (Fig. 3A). In the second approach, we measured astrocyte cellular processes or filopodia-like structures, which also demonstrated 37°C to be the optimal temperature (Fig. 3B). Intercellular communication and process formation may underlie important biological function at integral levels of function for astrocytes in whole organisms. If the in vitro results hold true in vivo, then the effect of temperature on these functions would be expected to affect biological neuronal function at a whole-organism level, which remains to be demonstrated.

The whole organism is a very complex system. Even tissues are quite complex, with thousands of parameters acting as multivariates against a single determinable parameter; hence, we require an understanding of some of the environmental effects on simpler systems, which the isolated cells represent. The integration of information derived from isolated systems may not add linearly but may provide important insight for appropriate fitting in an increasingly complex system of tissues, organs, or whole animals. Published studies render it abundantly clear that MS or demyelinating diseases are affected by environmental temperature (Leavitt et al., 2012; Meier and Christodoulou, 2012; Romberg et al., 2012). However, at present there is no suitable, well-characterized model system for determination of environmental effects, especially temperature, that can be readily translated into demyelinating diseases or MS. When model systems are developed, the information learned from isolated systems will be readily available for testing the hypothesis. Conversely, a potential in vitro system could be the use of astrocytes derived from MS or from an established spontaneous model of demyelination that captures MS-like features in ND4 (Mastronardi et al., 1993; Enriquez-Algeciras et al., 2011) or TCR2D2 (Bettelli et al., 2003) mice and control mice and subjecting them to environmental factors to characterize them with respect to deimination changes. Deimination has been implicated in neurodegenerative diseases (Asaga and Ishigami, 2001; Acharya et al., 2012; Jang et al., 2013) and glaucoma (Bhattacharya et al., 2006a,b). Deimination is a posttranslational modification in which protein-bound arginine is converted into citrulline by one of the PADs (Vossenaar et al., 2003). Our previous work with the retina and brain of a demyelinating mouse model provides some understanding of the occurrence of both hypo- and hyperdeimination in different cell types (Enriquez-Algeciras et al., 2013).

We have found hypodeimination to occur in neurons and hyperdeimination to be associated with astroglial cells. Therefore, assuming that those astrocytes were activated during the disease process and were hyperdeiminated as well, we wanted to investigate whether deimination could serve as a reactive astrocyte marker. We found that, in agreement with our hypothesis, the astrocytes exposed to higher incubation temperature demonstrated an increase in deimination as well as in the expression of PAD2, the enzyme responsible for this reaction. Our results suggest that astrocytes undergo two qualitatively different degrees of activation. One, at lower-temperature TSP, demonstrates an increased expression of TSP, AQP4, and S100β that shows an increase in expression of up to 40% at 31°C compared with the optimal normothermic condition of 37°C (Fig. 2). On the other hand, markers such as GFAP, ALDH1L, and J1-31 may undergo a progressive, up to 90% increase in expression from 31°C to 41°C. These groups of activation markers closely follow the increased expression pattern shown by cytoskeletal markers such as actin and lipid peroxidation product iso[4]LGE. PAD2 and deimination undergo a progressive increase with an increase in temperature from 31°C to 41°C, the lowest being at 31°C, suggesting that aberrant dysregulation associated with elevated deimination is more likely to occur under hyperthermic conditions than under hypothermic conditions. This is consistent with long-term complications found in MS patients subjected to hyperthermic conditions or hyperthermia treatment. The damaging effects of hyperthermia, usually accompanied by gliosis (Kim et al., 2014), and the beneficial effects of hypothermia, concomitant with reduced gliosis, have been shown after CNS injury or in degenerating diseases, such ischemic proliferative retinopathy (Rey-Funes et al., 2013). However, the genes or proteins underlying these damaging or protective processes remain completely unknown. The present work is a first step toward identifying proteins whose expression is altered because of changes in environmental temperatures. We envisage that this is the first step toward ascertaining the role of proteins or specific genes and their biological function with respect to temperature effects. Identification of astrocyte proteins when the cells are exposed to hypo- or hyperthermia will provide insight into their role in CNS function. Additional high-throughput genomic, proteomic, and metabolomic experiments will provide further information on and insight into the full spectrum of changes that astrocytes undergo as a consequence of changes in incubation temperature and will expand our understanding of underlying biochemical changes associated with changes in such environmental parameters.

REFERENCES

Acharya NK, Nagele EP, Han M, Coretti NJ, DeMarshall C, Kosciuk MC, Boulos PA, Nagele RG. 2012. Neuronal PAD4 expression and protein citrullination: possible role in production of autoantibodies associated with neurodegenerative disease. J Autoimmun 38:369–380.

Ahmed F, Torrado M, Johnson E, Morrison J, Tomarev SI. 2001. Changes in mRNA levels of the Myoc/Tigr gene in the rat eye after experimental elevation of intraocular pressure or optic nerve transection. Invest Ophthalmol Vis Sci 42:3165–3172.

Akiyama K, Sakurai Y, Asou H, Senshu T. 1999. Localization of peptidylarginine deiminase type II in a stage-specific immature oligodendrocyte from rat cerebral hemisphere. Neurosci Lett 274:53–55.

Algeciras, ME, Takahara H, Bhattacharya SK. 2008. Mechanical stretching elevates peptidyl arginine deiminase 2 expression in astrocytes. Curr Eye Res 33:994–1001.

Asaga H, Ishigami A. 2001. Protein deimination in the rat brain after kainate administration: citrulline-containing proteins as a novel marker of neurodegeneration. Neurosci Lett 299:5–8.

Berger JR, Sheremata W. 1982. The hot bath test and multiple sclerosis. JAMA 247:979.

Bettelli E, Pagany M, Weiner HL, Linington C, Sobel RA, Kuchroo VK. 2003. Myelin oligodendrocyte glycoprotein-specific T-cell receptor transgenic mice develop spontaneous autoimmune optic neuritis. J Exp Med 197:1073–1081.

Bhattacharya SK, Bhat MB, Takahara H. 2006a. Modulation of peptidyl arginine deiminase 2 and implication for neurodegeneration. Curr Eye Res 31:1063–1071.

Bhattacharya SK, Crabb JS, Bonilha VL, Gu X, Takahara H, Crabb JW. 2006b. Proteomics implicates peptidyl arginine deiminase 2 and optic nerve citrullination in glaucoma pathogenesis. Invest Ophthalmol Vis Sci 47:2508–2514.

Boesmans W, Rocha NP, Reis HJ, Holt M, Vanden Berghe P. 2014. The astrocyte marker Aldh1L1 does not reliably label enteric glial cells. Neurosci Lett 566:102–105.

Bradford CM, Ramos I, Cross AK, Haddock G, McQuaid S, Nicholas AP, Woodroofe MN. 2014. Localisation of citrullinated proteins in normal appearing white matter and lesions in the central nervous system in multiple sclerosis. J Neuroimmunol 273:85–95.

Enriquez-Algeciras M, Ding D, Chou TH, Wang J, Padgett KR, Porciatti V, Bhattacharya SK. 2011. Evaluation of a transgenic mouse model of multiple sclerosis with noninvasive methods. Invest Ophthalmol Vis Sci 52:2405–2411.

Enriquez-Algeciras M, Ding D, Mastronardi FG, Marc RE, Porciatti V, Bhattacharya SK. 2013. Deimination restores inner retinal visual function in murine demyelinating disease. J Clin Invest 123:646–656.

Flensner G, Ek AC, Soderhamn O, Landtblom AM. 2011. Sensitivity to heat in MS patients: a factor strongly influencing symptomology—an explorative survey. BMC Neurol 11:27.

Foo LC, Dougherty JD. 2013. Aldh1L1 is expressed by postnatal neural stem cells in vivo. Glia 61:1533–1541.

Froehler MT, Ovbiagele B. 2010. Therapeutic hypothermia for acute ischemic stroke. Expert Rev Cardiovasc Ther 8:593–603.

Garcia DM, Weigum SE, Koke JR. 2003. GFAP and nuclear lamins share an epitope recognized by monoclonal antibody J1-31. Brain Res 976:9–21.

Globus MY, Busto R, Lin B, Schnippering H, Ginsberg MD. 1995. Detection of free radical activity during transient global ischemia and recirculation: effects of intraischemic brain temperature modulation. J Neurochem 65:1250–1256.

Govindarajan, B, Junk A, Algeciras M, Salomon RG, Bhattacharya SK. 2009. Increased isolevuglandin-modified proteins in glaucomatous astrocytes. Mol Vis 15:1079–1091.

Gregorios JB, Mozes LW, Norenberg MD. 1985. Morphologic effects of ammonia on primary astrocyte cultures. II. Electron microscopic studies. J Neuropathol Exp Neurol 44:404–414.

Gruol DL, Nelson TE. 1997. Physiological and pathological roles of interleukin-6 in the central nervous system. Mol Neurobiol 15:307–339.

Guthrie TC, Nelson DA. 1995. Influence of temperature changes on multiple sclerosis: critical review of mechanisms and research potential. J Neurol Sci 129:1–8.

Jang B, Ishigami A, Maruyama N, Carp RI, Kim YS, Choi EK. 2013. Peptidylarginine deiminase and protein citrullination in prion diseases: strong evidence of neurodegeneration. Prion 7:42–46.

Jayakumar AR, Tong XY, Curtis KM, Ruiz-Cordero R, Shamaladevi N, Abuzamel M, Johnstone J, Gaidosh G, Rama Rao KV, Norenberg MD. 2014. Decreased astrocytic thrombospondin-1 secretion after chronic ammonia treatment reduces the level of synaptic proteins: in vitro and in vivo studies. J Neurochem 131:333–347.

Kim MJ, Cho JH, Cho JH, Park JH, Ahn JH, Tae HJ, Cho GS, Yan BC, Hwang IK, Lee CH, Bae EJ, Won MH, Lee JC. 2014. Impact of hyperthermia before and during ischemia–reperfusion on neuronal damage and gliosis in the gerbil hippocampus induced by transient cerebral ischemia. J Neurol Sci 348:101–110.

Kim WS, Halliday GM. 2012. Changes in sphingomyelin level affect alpha-synuclein and ABCA5 expression. J Parkinsons Dis 2:41–46.

Koike H, Sase K, Uchida H, Sudo T, Shiraiwa M, Sugawara K, Takahara H. 1994. Production and epitope specificity of monoclonal antibody against mouse peptidylarginine deiminase type II. Biosci Biotechnol Biochem 58:2286–2287.

Leavitt VM, Sumowski JF, Chiaravalloti N, Deluca J. 2012. Warmer outdoor temperature is associated with worse cognitive status in multiple sclerosis. Neurology 78:964–968.

Malhotra SK, Bhatnagar R, Shnitka TK, Herrera JJ, Koke JR, Singh MV. 1995. Rat glioma cell line as a model for astrogliosis. Cytobios 82: 39–51.

Martin ED, Araque A, Buno W. 2001. Synaptic regulation of the slow Ca^{2+}-activated K^{+} current in hippocampal CA1 pyramidal neurons: implication in epileptogenesis. J Neurophysiol 86:2878–2886.

Mastronardi FG, Ackerley CA, Arsenault L, Roots BI, Moscarello MA. 1993. Demyelination in a transgenic mouse: a model for multiple sclerosis. J Neurosci Res 36:315–324.

Meier DS, Christodoulou C. 2012. MS and heat: the smoke and the fire. Neurology 78:938–939.

Mowen KA, David M. 2014. Unconventional posttranslational modifications in immunological signaling. Nat Immunol 15:512–520.

Nesic O, et al. 2006. Acute and chronic changes in aquaporin 4 expression after spinal cord injury. Neuroscience 143:779–792.

Nicholas AP. 2013. Dual immunofluorescence study of citrullinated proteins in Alzheimer diseased frontal cortex. Neurosci Lett 545:107–111.

Okada-Ogawa A, Suzuki I, Sessle BJ, Chiang CY, Salter MW, Dostrovsky JO, Tsuboi Y, Kondo M, Kitagawa J, Kobayashi A, Noma N, Imamura Y, Iwata K. 2009. Astroglia in medullary dorsal horn (trigeminal spinal subnucleus caudalis) are involved in trigeminal neuropathic pain mechanisms. J Neurosci 29:11161–11171.

Parikh T, Eisner N, Venugopalan P, Yang Q, Lam BL, Bhattacharya SK. 2011. Proteomic analyses of corneal tissue subjected to alkali exposure. Invest Ophthalmol Vis Sci 52:1819–1831.

Pekny M, Nilsson M. 2005. Astrocyte activation and reactive gliosis. Glia 50:427–434.

Polderman KH, Herold I. 2009. Therapeutic hypothermia and controlled normothermia in the intensive care unit: practical considerations, side effects, and cooling methods. Crit Care Med 37:1101–1120.

Predy R, Malhotra SK, Das GD. 1988. Enhanced expression of a protein antigen (J1-31 antigen, 30 kilodaltons) by reactive astrocytes in lacerated spinal cord. J Neurosci Res 19:397–404, 466–467.

Rey-Funes M, Dorfman VB, Ibarra ME, Pena E, Contartese DS, Goldstein J, Acosta JM, Larrayoz IM, Martinez-Murillo R, Martinez A, Loidl CF. 2013. Hypothermia prevents gliosis and angiogenesis development in an experimental model of ischemic proliferative retinopathy. Invest Ophthalmol Vis Sci 54:2836–2846.

Ridet JL, Malhotra SK, Privat A, Gage FH. 1997. Reactive astrocytes: cellular and molecular cues to biological function. Trends Neurosci 20:570–577.

Romberg A, Ikonen A, Ruutiainen J, Virtanen A, Hamalainen P. 2012. The effects of heat stress on physical functioning in persons with multiple sclerosis. J Neurol Sci 319:42–46.

Salomon RG, Sha W, Brame C, Kaur K, Subbanagounder G, O'Neil J, Hoff HF, Roberts LJ. 1999. Protein adducts of iso[4]levuglandin E2, a product of the isoprostane pathway, in oxidized low density lipoprotein. J Biol Chem 274:20271–20280.

Sambandam T, Belousova M, Accaviti-Loper MA, Blanquicett C, Guercello V, Raijmakers R, Nicholas AP. 2004. Increased

peptidylarginine deiminase type II in hypoxic astrocytes. Biochem Biophys Res Commun 325:1324–1329.

Shuangshoti S, Thorner PS, Ruangvejvorachai P, Saha B, Groshen S, Taylor CR, Malhotra S, Imam SA. 2009. J1-31 protein expression in astrocytes and astrocytomas. Neuropathology 29:521–527.

Takahara H, Tsuchida M, Kusubata M, Akutsu K, Tagami S, Sugawara K. 1989. Peptidylarginine deiminase of the mouse. Distribution, properties, and immunocytochemical localization. J Biol Chem 264:13361–13368.

Terakawa H, Takahara H, Sugawara K. 1991. Three types of mouse peptidylarginine deiminase: characterization and tissue distribution. J Biochem 110:661–666.

Theodoric N, Bechberger JF, Naus CC, Sin WC. 2012. Role of gap junction protein connexin43 in astrogliosis induced by brain injury. PLoS One 7:e47311.

Vossenaar ER, Zendman AJ, van Venrooij WJ, Pruijn GJ. 2003. PAD, a growing family of citrullinating enzymes: genes, features and involvement in disease. Bioessays 25:1106–1118.

Wood DD, Bilbao JM, O'Connors P, Moscarello MA. 1996. Acute multiple sclerosis (Marburg type) is associated with developmentally immature myelin basic protein. Ann Neurol 40:18–24.

Wu TC, Grotta JC. 2013. Hypothermia for acute ischaemic stroke. Lancet Neurol 12:275–284.

Yu AC, Wu BY, Liu RY, Li Q, Li YX, Wong PF, Liu S, Lau LT, Fung YW. 2004. A model to induce low temperature trauma for in vitro astrogliosis study. Neurochem Res 29:2171–2176.

Zanotto C, Abib RT, Batassini C, Tortorelli LS, Biasibetti R, Rodrigues L, Nardin P, Hansen F, Gottfried C, Leite MC, Goncalves CA. 2013. Non-specific inhibitors of aquaporin-4 stimulate S100B secretion in acute hippocampal slices of rats. Brain Res 1491:14–22.

Zhang S, Zis O, Ly PT, Wu Y, Zhang S, Zhang M, Cai F, Bucala R, Shyu WC, Song W. 2014. Downregulation of MIF by NFkappaB under hypoxia accelerated neuronal loss during stroke. FASEB J 28:4394–4407.

Zhao J, Moore AN, Clifton GL, Dash PK. 2005. Sulforaphane enhances aquaporin-4 expression and decreases cerebral edema following traumatic brain injury. J Neurosci Res 82:499–506.